Remarks on the numerical solution of the adjoint quasi-one-dimensional Euler equations

ARTICLE *in* INTERNATIONAL JOURNAL FOR NUMERICAL METHODS IN FLUIDS · JUNE 2012

Impact Factor: 1.24 · DOI: 10.1002/fld.2621

2 AUTHORS:

Carlos Lozano
Instituto Nacional de Técnica Aeroespacial
37 PUBLICATIONS **234** CITATIONS
SEE PROFILE

Jorge Ponsin
Instituto Nacional de Técnica Aeroespacial
9 PUBLICATIONS **24** CITATIONS
SEE PROFILE

REMARKS ON THE NUMERICAL SOLUTION OF THE ADJOINT QUASI-ONE-DIMENSIONAL EULER EQUATIONS*

C. Lozano†‡ and J. Ponsin

Fluid Dynamics Branch, National Institute for Aerospace Technology
Carretera de Ajalvir, Km., 28850 Torrejón de Ardoz, Spain

SUMMARY

We examine the numerical solution of the adjoint quasi-one-dimensional Euler equations with a central-difference finite volume scheme with JST dissipation, for both the continuous and discrete approaches. First, complete formulations and discretization of the quasi-one-dimensional Euler equations, the continuous adjoint equation and its counterpart the discrete adjoint equation are reviewed. The differences between the continuous and discrete boundary conditions are also explored. Second, numerical testing is carried out on a symmetric converging-diverging duct under subsonic flow conditions. This analysis reveals that the discrete adjoint scheme, while being manifestly less accurate than the continuous approach, gives nevertheless more accurate flow sensitivities.

KEY WORDS: adjoint equation; design optimization

1. INTRODUCTION

For the past 20 years, there has been an increasing interest in the application of adjoint methods in Computational Fluid Dynamics developments. Originally introduced in the CFD arena by Jameson within the context of optimal aerodynamic shape design [1-4], this technique has been extended to deal with error analysis and grid adaptation [5-7].

In design applications, the adjoint solution provides the sensitivities of an objective function such as lift or drag to a number of design variables which parameterize the

* Final version to appear in *Int. J. Numer. Meth. Fluids*, 2011.
† Correspondence to: C. Lozano, Fluid Dynamics Branch, National Institute for Aerospace Technology, Carretera de Ajalvir, Km., 28850 Torrejón de Ardoz, Spain.
‡ E-mail: lozanorc@inta.es

shape. These sensitivities can then be used to set up an optimization procedure. In the error control context, the adjoint solution provides the sensitivity of the objective function to errors in the flow discretization. This information can then be used to obtain a-posteriori error estimates or to perform adaptive mesh (de)refinement.

From a mathematical viewpoint, the (analytic) adjoint equations are obtained from the linearization of the flow equations. For numerical applications, a discretized version of the adjoint equations is required, which can be formulated in two ways, either by discretizing the analytic adjoint equations (the so-called *continuous* approach), or by linearizing the discretized flow equations (the *discrete* approach). As the operations of linearization and discretization do not commute in general, sensitivity derivatives obtained by using the two approaches may not be identical, with discrete adjoint gradients being consistent with finite-difference gradients independent of the mesh size.

On the other hand, the continuous adjoint method has the advantage that the adjoint system has a unique formulation which does not depend on the numerical scheme used to solve the flow equations. A comparison between both approaches has shown that in typical shape optimization problems the differences do not have a significant effect on the final result [8]. However, design applications usually focus on the sensitivity derivatives and not on the adjoint solutions themselves, partly owing to the lack of exact solutions for the adjoint equations, so there is usually little information concerning the comparison between continuous and discrete adjoint solutions.

Quasi-1D flows are interesting because, while retaining some of the features of more complex flows (such as non-linearities, shocks, etc), they are nevertheless simple enough to possess computable exact solutions for both the flow and adjoint equations under very generic circumstances [9]. In the present study both, the continuous and discrete adjoint approaches, are examined and compared for a standard discretization of the quasi-1D Euler equations (a central-difference finite-volume scheme with JST artificial dissipation, which is routinely used in industrial flow solvers). Especial emphasis is put on the derivation of the adjoint boundary conditions (section 3) because this is a key point for the continuous approach implementation, as well as to the detailed comparison of the continuous and discrete solvers, both in terms of the resulting numerical schemes and the accuracy of the solutions.

2. ADJOINT QUASI-ONE-DIMENSIONAL EULER EQUATIONS

2.1 Flow Equations

The quasi-one-dimensional Euler equations for steady flow in a duct of cross-section $h(x)$, on the interval $-1 \le x \le 1$, read [9-11]

$$R(U,h) = \frac{d}{dx}\left(hF\right) - \frac{dh}{dx}\mathrm{P} = 0, \tag{1}$$

where

$$U = \begin{pmatrix} \rho \\ \rho u \\ \rho E \end{pmatrix}, \quad F = \begin{pmatrix} \rho u \\ \rho u^2 + P \\ \rho u H \end{pmatrix}, \quad \mathrm{P} = \begin{pmatrix} 0 \\ P \\ 0 \end{pmatrix} \tag{2}$$

Here, ρ is the density, u is the velocity, P is the pressure, E is the total energy and H is the stagnation enthalpy. The system is closed by the equation of state for an ideal gas

$$P = (\gamma - 1)\rho\left[E - \frac{1}{2}u^2\right], \quad H = E + \frac{P}{\rho} = \frac{\gamma}{\gamma - 1}\frac{P}{\rho} + \frac{1}{2}u^2 \tag{3}$$

2.2 Adjoint Equations

Linearization of the flow equations with respect to perturbations in the flow solution, δU, and the geometry, δh, which are of relevance to design applications, produces

$$\frac{d}{dx}\left(hA\delta U\right) - \frac{dh}{dx}B\delta U = \frac{d\delta h}{dx}\mathrm{P} - \frac{d}{dx}\left(\delta h F\right), \tag{4}$$

where $A = \partial F/\partial U$ and $B = \partial \mathrm{P}/\partial U$. For error analysis applications, the right hand side (RHS) of Eq. (4) is replaced by the truncation error.

The derivation of the adjoint equations requires, in the first place, specifying an objective or cost function, which in this work is chosen to be the integral of the pressure along the duct,

$$J = \int_{-1}^{1} P dx \tag{5}$$

The perturbation to the cost function (5) due to changes in the flow and the geometry is simply

$$\delta J = \int_{-1}^{1} \frac{\partial P}{\partial U} \delta U dx \tag{6}$$

The variation (6) can be computed without actually solving (4) for each independent perturbation. Introducing the adjoint state Ψ as a Lagrange multiplier to enforce the flow equations (1), the augmented cost function is

$$J = \int_{-1}^{1} P dx - \int_{-1}^{1} \Psi^T R(U,h) dx \tag{7}$$

which is equal to (5) under the assumption that $R(U,h) = 0$. Linearizing J with respect to U and h gives

$$\delta J = \int_{-1}^{1} \frac{\partial P}{\partial U} \delta U dx - \int_{-1}^{1} \Psi^T \left[\frac{d}{dx}\left(hA\delta U\right) - \frac{dh}{dx} B\delta U - \frac{d\delta h}{dx} \mathrm{P} - \frac{d}{dx}\left(\delta h F\right) \right] dx \tag{8}$$

After integration by parts and rearrangement, this yields

$$\begin{aligned} \delta J = & \int_{-1}^{1} \Psi^T \left[\frac{d\delta h}{dx} \mathrm{P} - \frac{d}{dx}\left(\delta h F\right) \right] dx \\ & - \int_{-1}^{1} \delta U^T \left[-hA^T \frac{d\Psi}{dx} - \frac{dh}{dx} B^T \Psi - \frac{\partial P}{\partial U}^T \right] dx - \left[h\Psi^T A\delta U \right]_{-1}^{1} \end{aligned} \tag{9}$$

Eq. (9) holds valid for any value of the multiplier Ψ, so we are free to choose it to simplify the resulting expressions. By choosing Ψ in such a way that

$$-hA^T \frac{d\Psi}{dx} - \frac{dh}{dx} B^T \Psi - \frac{\partial P}{\partial U}^T = 0 \tag{10}$$

and

$$\left[h\Psi^T A\delta U \right]_{-1}^{1} = 0 \tag{11}$$

δJ can be computed by the remaining terms of (9)

$$\delta J = \int_{-1}^{1} \Psi^T \left[\frac{d\delta h}{dx} \mathrm{P} - \frac{d}{dx}\left(\delta h F\right) \right] dx \tag{12}$$

independently of δU and hence of the number of design variables. Eq. (10) is the adjoint equation, while Eq. (11) gives the inlet and exit boundary conditions for the

adjoint problem. At a boundary where the flow equations have n incoming characteristics, and hence n imposed boundary conditions, the adjoint equations will thus have $(3 - n)$ boundary conditions corresponding to an equal number of incoming adjoint characteristics.

3. BOUNDARY CONDITIONS

We will now illustrate the derivation of the adjoint boundary conditions. We will restrict ourselves to subsonic flow conditions.

3.1. Subsonic Inlet ($x = -1$)

There are two incoming characteristics (with eigenvalues u, $u + c$) and one outgoing characteristic (with eigenvalue $u - c.$) Here $c = \sqrt{\gamma(P/\rho)}$ is the speed of sound. For the flow equations, two physical boundary conditions and one numerical boundary condition must be specified. A possible choice is to fix the stagnation enthalpy H and total pressure $P_t = P\left(1 + \frac{\gamma-1}{2} M^2\right)^{\frac{\gamma}{\gamma-1}}$ to their free stream values, and to extrapolate the Mach number M from the interior. On the other hand, the boundary conditions for the adjoint problem are defined so as to enforce

$$h\Psi^T A\delta U\Big|_{x=-1} = 0 \tag{13}$$

Expanding (13) in terms of the inlet variables $\left(H, P_t, M\right)$

$$\Psi^T A\delta U = \Psi^T \frac{\partial F}{\partial H}\bigg|_{P_t, M} \delta H + \Psi^T \frac{\partial F}{\partial P_t}\bigg|_{H, M} \delta P_t + \Psi^T \frac{\partial F}{\partial M}\bigg|_{H, P_t} \delta M \tag{14}$$

and noting that $\delta H = \delta H_\infty$ and $\delta P_t = \delta P_{t\infty}$ are both zero if the free-stream values are held fixed, we see that the remaining dependence of (13) on δM can be removed with the following adjoint boundary condition

$$\Psi^T \frac{\partial F}{\partial M}\bigg|_{H, P_t} = 0. \tag{15}$$

To actually implement the inlet boundary condition in a numerical solver, we have to impose (15) and extrapolate two other independent combinations of the adjoint

variables from the interior of the domain. We do this by defining adjoint inlet variables $\tilde{\Psi}_{in} = \left(\tilde{\psi}_M, \tilde{\psi}_H, \tilde{\psi}_{P_t}\right)^T$, as follows

$$\begin{aligned}
\tilde{\psi}_M &= \frac{M\left(1+\frac{\gamma-1}{2}M^2\right)}{\rho u\left(1-M^2\right)}\left(\frac{\partial F}{\partial M}\right)^T_{H,P_t}\Psi = \psi_1 + u\psi_2 + H\psi_3, \\
\tilde{\psi}_H &= \frac{2H}{\rho u}\left(\frac{\partial F}{\partial H}\right)^T_{M,P_t}\Psi = -\psi_1 + H\psi_3, \\
\tilde{\psi}_{P_t} &= P_t\left(\frac{\partial F}{\partial P_t}\right)^T_{H,M}\Psi = \rho u\psi_1 + \left(\rho u^2 + P\right)\psi_2 + \rho u H\psi_3
\end{aligned} \tag{16}$$

In the new variables, the inlet boundary conditions imply that $\tilde{\psi}_M = 0,$ while $\tilde{\psi}_H$ and $\tilde{\psi}_{P_t}$ are extrapolated from the interior of the domain. Inverting Eq. (16) gives the final relation

$$\Psi_{in} = \begin{pmatrix}\psi_1\\ \psi_2\\ \psi_3\end{pmatrix}_{in} = \begin{pmatrix} \frac{\rho u^2+P}{2P} & -\frac{1}{2} & -\frac{u}{2P} \\ -\frac{\rho u}{P} & 0 & \frac{1}{P} \\ \frac{\rho u^2+P}{2PH} & \frac{1}{2H} & -\frac{u}{2PH}\end{pmatrix}\begin{pmatrix}0\\ \tilde{\psi}^{(e)}_H\\ \tilde{\psi}^{(e)}_{P_t}\end{pmatrix} = \begin{pmatrix} -\frac{1}{2}\tilde{\psi}^{(e)}_H - \frac{u}{2P}\tilde{\psi}^{(e)}_{P_t} \\ \frac{1}{P}\tilde{\psi}^{(e)}_{P_t} \\ \frac{1}{2H}\tilde{\psi}^{(e)}_H - \frac{u}{2PH}\tilde{\psi}^{(e)}_{P_t}\end{pmatrix}. \tag{17}$$

Eq. (17) can be written in a more compact way in terms of the extrapolated adjoint state $\Psi^{(e)}_{in} = 2\Psi_{j=0} - \Psi_{j=1}$ (or $\Psi^{(e)}_{in} = \Psi_{j=0}$ if a zeroth-order extrapolation is picked) as follows

$$\Psi_{in} = \frac{1}{\left|\frac{\partial F}{\partial(M,H,P_t)}\right|}\left[\left(\frac{\partial F}{\partial P_t}\times\frac{\partial F}{\partial M}\right)\left(\frac{\partial F}{\partial H}^T\cdot\Psi^{(e)}_{in}\right) + \left(\frac{\partial F}{\partial M}\times\frac{\partial F}{\partial H}\right)\left(\frac{\partial F}{\partial P}^T\cdot\Psi^{(e)}_{in}\right)\right] =$$

$$\Psi^{(e)}_{in} - \frac{1}{\left|\frac{\partial F}{\partial(M,H,P_t)}\right|}\left(\frac{\partial F}{\partial H}\times\frac{\partial F}{\partial P_t}\right)\left(\frac{\partial F}{\partial M}^T\cdot\Psi^{(e)}_{in}\right) = \tag{18}$$

$$\Psi^{(e)}_{in} - \frac{\partial M}{\partial F}^T\left(\frac{\partial F}{\partial M}^T\cdot\Psi^{(e)}_{in}\right)$$

where $\left|\frac{\partial F}{\partial(M,H,P_t)}\right| = \det\left(\frac{\partial F}{\partial(M,H,P_t)}\right)$, $\frac{\partial F}{\partial X}\times\frac{\partial F}{\partial Y} = \varepsilon_{abc}\frac{\partial F^b}{\partial X}\frac{\partial F^c}{\partial Y}$ for any two variables X and Y, ε_{abc} is the permutation tensor and $a,b,c = 1,\ldots,3.$

3.2. Subsonic Exit ($x=1$)

There is one incoming characteristic (with eigenvalue $u-c$) and two outgoing characteristics (with eigenvalues $u,\ u+c$). One physical boundary condition and two numerical boundary conditions have to be enforced for the flow equations. A typical choice is to set the exit pressure P equal to the free stream pressure P_∞, and to extrapolate two other variables (such as ρ and u, for example) from the interior. The boundary conditions for the adjoint problem are defined so as to enforce

$$h\Psi^T A\delta U\Big|_{x=1}=0 \tag{19}$$

Expanding (19) in terms of the exit variables (ρ,u,P)

$$\Psi^T A\delta U=\Psi^T\left.\frac{\partial F}{\partial\rho}\right|_{P,u}\delta\rho+\Psi^T\left.\frac{\partial F}{\partial u}\right|_{P,\rho}\delta u+\Psi^T\left.\frac{\partial F}{\partial P}\right|_{\rho,u}\delta P \tag{20}$$

and noting that $\delta P=\delta P_\infty$ is zero if the free-stream pressure is held fixed, removing the final dependence of (19) on $\delta\rho,\delta u$ demands the adjoint boundary conditions

$$\begin{aligned}\Psi^T\left.\frac{\partial F}{\partial\rho}\right|_{p,u}&=0,\\ \Psi^T\left.\frac{\partial F}{\partial u}\right|_{p,\rho}&=0.\end{aligned} \tag{21}$$

With Eq. (21) the new adjoint variables for the exit boundary condition read

$$\tilde\Psi_{out}=\begin{pmatrix}\tilde\psi_\rho\\ \tilde\psi_u\\ \tilde\psi_p\end{pmatrix}=\begin{pmatrix}u^{-1}\left(\partial F/\partial\rho\right)^T\Psi\\ \rho^{-1}\left(\partial F/\partial u\right)^T\Psi\\ \left(\partial F/\partial p\right)^T\Psi\end{pmatrix}=\begin{pmatrix}1 & u & u^2/2\\ 1 & 2u & H+u^2\\ 0 & 1 & \frac{\gamma}{\gamma-1}u\end{pmatrix}\begin{pmatrix}\psi_1\\ \psi_2\\ \psi_3\end{pmatrix}. \tag{22}$$

In the new variables, exit boundary conditions read $\tilde\psi_\rho=\tilde\psi_u=0,$ while $\tilde\psi_P$ is extrapolated from the interior of the domain. In the original adjoint variables this yields

$$\Psi_{out}=\begin{pmatrix}\psi_1\\ \psi_2\\ \psi_3\end{pmatrix}_{out}=\frac{1}{\Delta}\begin{pmatrix}\frac{u^2(\gamma+1)-H(\gamma-1)}{\gamma-1} & -\frac{u^2}{2}\frac{\gamma+1}{\gamma-1} & uH\\ -\frac{\gamma u}{\gamma-1} & \frac{\gamma u}{\gamma-1} & -\left(H+\frac{u^2}{2}\right)\\ 1 & -1 & u\end{pmatrix}\begin{pmatrix}0\\ 0\\ \tilde{\psi}_P^{(e)}\end{pmatrix}=\begin{pmatrix}\frac{uH}{\Delta}\tilde{\psi}_P^{(e)}\\ -\frac{H+\frac{u^2}{2}}{\Delta}\tilde{\psi}_P^{(e)}\\ \frac{u}{\Delta}\tilde{\psi}_P^{(e)}\end{pmatrix}, \qquad (23)$$

where $\Delta=\frac{\gamma}{\gamma-1}u^2-H-\frac{u^2}{2}$. As above, Eq. (23) can be written more compactly as follows

$$\Psi_{out}=\frac{1}{\left|\frac{\partial F}{\partial(\rho,u,P)}\right|}\left(\frac{\partial F}{\partial\rho}\times\frac{\partial F}{\partial u}\right)\left(\frac{\partial F}{\partial P}^T\cdot\Psi_{out}^{(e)}\right)=$$

$$\Psi_{out}^{(e)}-\frac{1}{\left|\frac{\partial F}{\partial(\rho,u,P)}\right|}\left[\left(\frac{\partial F}{\partial u}\times\frac{\partial F}{\partial P}\right)\left(\frac{\partial F}{\partial\rho}^T\cdot\Psi_{out}^{(e)}\right)+\left(\frac{\partial F}{\partial P}\times\frac{\partial F}{\partial\rho}\right)\left(\frac{\partial F}{\partial u}^T\cdot\Psi_{out}^{(e)}\right)\right]= \qquad (24)$$

$$\Psi_{out}^{(e)}-\frac{\partial\rho}{\partial F}^T\left(\frac{\partial F}{\partial\rho}^T\cdot\Psi_{out}^{(e)}\right)-\frac{\partial u}{\partial F}^T\left(\frac{\partial F}{\partial u}^T\cdot\Psi_{out}^{(e)}\right)$$

where $\Psi_{out}^{(e)}=2\Psi_{j=n_e-1}-\Psi_{j=n_e-2}$ for a first-order extrapolation (or $\Psi_{out}^{(e)}=\Psi_{j=n_e-1}$ for zeroth-order extrapolation).

Numerous authors have considered in detail the issue of the adjoint boundary conditions [10,12,13]. The advantage of the procedure described above, which can be readily carried over to more general situations involving different prescribed variables, different number of incoming/outgoing characteristics or boundary types, is that it gives closed expressions as (17) and (23) for the boundary adjoint variables which comprise both the physical and numerical boundary conditions in an unambiguous way.

4. NUMERICAL IMPLEMENTATION

4.1. Flow solver

The flow equations are discretized using a finite-volume, cell-centered scheme. Our conventions for cell and face indices are sketched in Fig. 1 below.

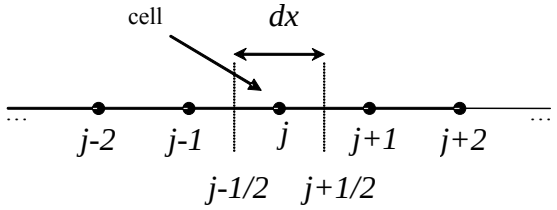

Fig. 1. Scheme of computational mesh

We use a central scheme with JST-type artificial dissipation [14]. At an interior cell, the numerical residual takes the form

$$R_j = C_{j+\frac{1}{2}} - C_{j-\frac{1}{2}} - \left(D_{j+\frac{1}{2}} - D_{j-\frac{1}{2}} \right) - S_j \tag{25}$$

where

$$C_{j\pm\frac{1}{2}} = \frac{1}{2} h_{j\pm\frac{1}{2}} \left(F_j + F_{j\pm1} \right) \tag{26}$$

is the conservative flux at face $j-\frac{1}{2}$, with $h_{j-\frac{1}{2}} \equiv h(x_{j-\frac{1}{2}})$ being the duct's cross-section at the face and F_j the flux vector (as in eq. (2)) at cell j. The artificial dissipation scheme is defined as

$$D_{j-\frac{1}{2}} = h_{j-\frac{1}{2}} \left(\varepsilon^{(2)}_{j-\frac{1}{2}} \lambda_{j-\frac{1}{2}} (U_j - U_{j-1}) - \varepsilon^{(4)}_{j-\frac{1}{2}} \lambda_{j-\frac{1}{2}} (U_{j+1} - 3U_j + 3U_{j-1} - U_{j-2}) \right) \tag{27}$$

with

$$\begin{aligned} \varepsilon^{(2)}_{j-\frac{1}{2}} &= k_2 \max(\nu_j, \nu_{j-1}), \\ \nu_j &= \left| \frac{P_{j+1} - 2P_j + P_{j-1}}{P_{j+1} + 2P_j + P_{j-1}} \right|, \\ \varepsilon^{(4)}_{j-\frac{1}{2}} &= \max(0, k_4 - \varepsilon^{(2)}_{j-\frac{1}{2}}), \\ \lambda_{j-\frac{1}{2}} &= \left((u_j + c_j) + (u_{j-1} + c_{j-1}) \right) \big/ 2 \end{aligned} \tag{28}$$

where c_j is the speed of sound at cell j, and the parameters take the typical values $k_2 = 1/2, \quad k_4 = 1/64$. Finally, the source term S_j is simply

$$S_j = \begin{pmatrix} 0 \\ P_j \\ 0 \end{pmatrix} \left(h_{j+\frac{1}{2}} - h_{j-\frac{1}{2}} \right). \tag{29}$$

Boundary conditions are imposed weakly, by modifying the residual at the boundaries, as follows (cell indices run from 0 to $n_e - 1$, while face indices run from $-1/2$ to $n_e + 1/2$)

$$\begin{aligned} &\textit{Inlet} \\ &C_{-\frac{1}{2}} = h_{-\frac{1}{2}} F(U_{in}), \\ &D_{-\frac{1}{2}} = h_{\frac{1}{2}} \left(\varepsilon^{(2)}_{\frac{1}{2}} \lambda_{\frac{1}{2}} (U_1 - U_0) \right), \\ &D_{\frac{1}{2}} = h_{\frac{1}{2}} \left(\varepsilon^{(2)}_{\frac{1}{2}} \lambda_{\frac{1}{2}} (U_1 - U_0) - \varepsilon^{(4)}_{\frac{1}{2}} \lambda_{\frac{1}{2}} (U_2 - 3U_1 + 3U_0 - U_{-1}) \right), \end{aligned} \tag{30}$$

where $U_{-1} = 2U_0 - U_1$ and U_{in} is defined by $(M_{in}, H_\infty, P_{t\infty})$, where $M_{in} = 2\frac{u_0}{c_0} - \frac{u_1}{c_1}$.

Exit

$$
\begin{aligned}
&C_{n_e-\frac{1}{2}} = h_{n_e-\frac{1}{2}} F(U_{out}),\\
&D_{n_e-\frac{1}{2}} = h_{n_e-\frac{1}{2}} \left(\varepsilon^{(2)}_{n_e-\frac{3}{2}} \lambda_{n_e-\frac{3}{2}} (U_{n_e-1} - U_{n_e-2}) \right),\\
&D_{n_e-\frac{3}{2}} = h_{n_e-\frac{3}{2}} \left(\varepsilon^{(2)}_{n_e-\frac{3}{2}} \lambda_{n_e-\frac{3}{2}} (U_{n_e-1} - U_{n_e-2}) - \varepsilon^{(4)}_{n_e-\frac{3}{2}} \lambda_{n_e-\frac{3}{2}} (U_{n_e} - 3U_{n_e-1} + 3U_{n_e-2} - U_{n_e-3}) \right),
\end{aligned}
\tag{31}
$$

where $U_{n_e} = 2U_{n_e-1} - U_{n_e-2}$ and U_{out} is defined by $(\rho_{out}, u_{out}, P_\infty)$, , where $\rho_{out} = 2\rho_{n_e-1} - \rho_{n_e-2}$ and $u_{out} = 2u_{n_e-1} - u_{n_e-2}$.

4.2. Continuous adjoint solver

To solve the continuous adjoint equation (10), we use a discretization scheme similar to that used for the Euler equations. At an interior cell, the numerical residual takes the form

$$
R^{adj}_j = -C^{adj}_j - \left(D^{adj}_{j+\frac{1}{2}} - D^{adj}_{j-\frac{1}{2}} \right) - S^{adj}_j \tag{32}
$$

The convective flux takes the form

$$
C^{adj}_j = A^T_j \left(\Phi_{j+\frac{1}{2}} - \Phi_{j-\frac{1}{2}} - \left(h_{j+\frac{1}{2}} - h_{j-\frac{1}{2}} \right) \Psi_j \right), \tag{33}
$$

where

$$
\Phi_{j\pm\frac{1}{2}} = \frac{1}{2} h_{j\pm\frac{1}{2}} \left(\Psi_j + \Psi_{j\pm1} \right) \tag{34}
$$

and A^T_j is the flux jacobian at cell j. Notice that the above discretization (33) is manifestly non-conservative, in accordance with the character of the analytic adjoint equation (10). The artificial dissipation scheme is defined as

$$
D^{adj}_{j-\frac{1}{2}} = h_{j-\frac{1}{2}} \left(\varepsilon^{(2)}_{j-\frac{1}{2}} \lambda_{j-\frac{1}{2}} (\Psi_j - \Psi_{j-1}) - \varepsilon^{(4)}_{j-\frac{1}{2}} \lambda_{j-\frac{1}{2}} (\Psi_{j+1} - 3\Psi_j + 3\Psi_{j-1} - \Psi_{j-2}) \right) \tag{35}
$$

where $\varepsilon^{(2)}_{j-\frac{1}{2}}, \varepsilon^{(4)}_{j-\frac{1}{2}}, \lambda_{j-\frac{1}{2}}$ are as in Eq. (28) with $k_2 = 1/2$, $k_4 = 1/64$. Finally, the source term S^{adj}_j is simply

$$S_j^{adj} = \left((x_{j+\frac{1}{2}} - x_{j-\frac{1}{2}}) + (h_{j+\frac{1}{2}} - h_{j-\frac{1}{2}})\psi_{2,j} \right) \frac{\partial P}{\partial U}^T \tag{36}$$

Boundary conditions are imposed by modifying the residual at the boundaries, as follows

Inlet

$$\begin{aligned}
&\Phi_{-\frac{1}{2}} = h_{-\frac{1}{2}} \Psi_{in}, \\
&D_{-\frac{1}{2}}^{adj} = h_{\frac{1}{2}} \left(\varepsilon_{\frac{1}{2}}^{(2)} \lambda_{\frac{1}{2}} (\Psi_1 - \Psi_0) \right), \\
&D_{\frac{1}{2}}^{adj} = h_{\frac{1}{2}} \left(\varepsilon_{\frac{1}{2}}^{(2)} \lambda_{\frac{1}{2}} (\Psi_1 - \Psi_0) - \varepsilon_{\frac{1}{2}}^{(4)} \lambda_{\frac{1}{2}} (\Psi_2 - 3\Psi_1 + 3\Psi_0 - \Psi_{-1}) \right), \\
&\Psi_{-1} = 2\Psi_0 - \Psi_1,
\end{aligned} \tag{37}$$

and

Exit

$$\begin{aligned}
&\Phi_{n_e - \frac{1}{2}} = h_{n_e - \frac{1}{2}} \Psi_{out}, \\
&D_{n_e - \frac{1}{2}} = h_{n_e - \frac{3}{2}} \left(\varepsilon_{n_e - \frac{3}{2}}^{(2)} \lambda_{n_e - \frac{3}{2}} (\Psi_{n_e - 1} - \Psi_{n_e - 2}) \right), \\
&D_{n_e - \frac{3}{2}} = h_{n_e - \frac{3}{2}} \left(\varepsilon_{n_e - \frac{3}{2}}^{(2)} \lambda_{n_e - \frac{3}{2}} (\Psi_{n_e - 1} - \Psi_{n_e - 2}) - \varepsilon_{n_e - \frac{3}{2}}^{(4)} \lambda_{n_e - \frac{3}{2}} (\Psi_{n_e} - 3\Psi_{n_e - 1} + 3\Psi_{n_e - 2} - \Psi_{n_e - 3}) \right), \\
&\Psi_{n_e} = 2\Psi_{n_e - 1} - \Psi_{n_e - 2},
\end{aligned} \tag{38}$$

where in and out states are computed from (17) and (23)

In

$$\begin{aligned}
&\Psi_{in} = \begin{pmatrix} -\frac{1}{2} & -\frac{u}{2P} \\ 0 & \frac{1}{P} \\ \frac{1}{2H} & -\frac{u}{2PH} \end{pmatrix}_{j=0} \begin{pmatrix} 2\tilde{\psi}_{H,j=0} - \tilde{\psi}_{H,j=1} \\ 2\tilde{\psi}_{P_t,j=0} - \tilde{\psi}_{P_t,j=1} \end{pmatrix}, \\
&\tilde{\psi}_{H,j} = -\psi_{1,j} + H\psi_{3,j}, \\
&\tilde{\psi}_{P_t,j} = \rho u \psi_{1,j} + \left(\rho u^2 + P \right) \psi_{2,j} + \rho u H \psi_{3,j},
\end{aligned}$$

Out

$$\begin{aligned}
&\Psi_{out} = (2\tilde{\psi}_{p,j=n_e-1} - \tilde{\psi}_{p,j=n_e-2}) \begin{pmatrix} \frac{uH}{\Delta} \\ -\frac{H + \frac{u^2}{2}}{\Delta} \\ \frac{u}{\Delta} \end{pmatrix}_{j=n_e-1} \\
&\tilde{\psi}_p = \psi_{2,j} + \frac{\gamma}{\gamma - 1} u \psi_{3,j}, \\
&\Delta = \frac{\gamma}{\gamma - 1} u^2 - H - \frac{u^2}{2}
\end{aligned} \tag{39}$$

4.3. Discrete adjoint solver

The discrete adjoint equations can be written as

$$\frac{\partial J_{disc}}{\partial U_i} = 0 \tag{40}$$

where $i = 0,\ldots,n_e - 1$ and J_{disc} is the discrete form of the augmented objective function (7)

$$J_{disc} = \sum_{j=0}^{n_e-1} P_j \left(x_{j+\frac{1}{2}} - x_{j-\frac{1}{2}} \right) - \sum_{j=0}^{n_e-1} \Psi_j^T R_j \tag{41}$$

Where R_j is the numerical flow residual. Carrying out the derivatives and rearranging yields the discrete adjoint residual

$$R_i^{dadj} = \sum_j \left(\frac{\partial R_j}{\partial U_i} \right)^T \Psi_j - \left(\frac{\partial P_i}{\partial U_i} \right)^T \left(x_{i+\frac{1}{2}} - x_{i-\frac{1}{2}} \right) \tag{42}$$

Applying (42) to the flow solver residual (25)–(31) yields the following discrete adjoint residuals

$$R_j^{dadj} = C_j^{dadj} + D_j^{dadj} - S_j^{dadj} - J_j^{dadj} \tag{43}$$

where

$$\begin{aligned}
C_j^{dadj} &= -\frac{1}{2} A_j^T \left(h_{j+\frac{1}{2}} \left(\Psi_{j+1} - \Psi_j \right) + h_{j-\frac{1}{2}} \left(\Psi_j - \Psi_{j-1} \right) \right) \\
D_j^{dadj} &= -\kappa_{j+\frac{1}{2}}^{(2)} (\Psi_{j+1} - \Psi_j) + (\kappa_{j+\frac{3}{2}}^{(4)} \Psi_{j+2} - 3\kappa_{j+\frac{1}{2}}^{(4)} \Psi_{j+1} + 3\kappa_{j-\frac{1}{2}}^{(4)} \Psi_j - \kappa_{j-\frac{3}{2}}^{(4)} \Psi_{j-1}) \\
&+ \kappa_{j-\frac{1}{2}}^{(2)} (\Psi_j - \Psi_{j-1}) - (\kappa_{j+\frac{3}{2}}^{(4)} \Psi_{j+1} - 3\kappa_{j+\frac{1}{2}}^{(4)} \Psi_j + 3\kappa_{j-\frac{1}{2}}^{(4)} \Psi_{j-1} - \kappa_{j-\frac{3}{2}}^{(4)} \Psi_{j-2}) \\
S_j^{dadj} &= \left(\frac{\partial S_j}{\partial U_j} \right)^T \Psi_j = \left(\frac{\partial P_j}{\partial U_j} \right)^T \left(h_{j+\frac{1}{2}} - h_{j-\frac{1}{2}} \right) \Psi_{2,j} \\
J_j^{dadj} &= \left(\frac{\partial P_j}{\partial U_j} \right)^T \left(x_{j+\frac{1}{2}} - x_{j-\frac{1}{2}} \right)
\end{aligned} \tag{44}$$

and

$$\begin{aligned}
\kappa_{j-\frac{1}{2}}^{(2)} &= h_{j-\frac{1}{2}} \varepsilon_{j-\frac{1}{2}}^{(2)} \lambda_{j-\frac{1}{2}} \\
\kappa_{j-\frac{1}{2}}^{(4)} &= h_{j-\frac{1}{2}} \varepsilon_{j-\frac{1}{2}}^{(4)} \lambda_{j-\frac{1}{2}} \\
A_j^T &= \left(\frac{\partial F_j}{\partial U_j} \right)^T
\end{aligned} \tag{45}$$

Notice that the flow-dependent dissipation factors $\varepsilon^{(2)}_{j-\frac{1}{2}}, \varepsilon^{(4)}_{j-\frac{1}{2}}$ and $\lambda_{j-\frac{1}{2}}$ have been treated as constants. The dissipation parameters have the typical values $k_2 = 1/2, \quad k_4 = 1/64$ (as in the flow solver).

At inlet and exit boundaries the above residuals get modified following the structure of the flow solver boundary residuals

Inlet

$$
\begin{aligned}
C_0^{dadj} &= -\frac{1}{2} A_0^T h_{\frac{1}{2}} \left(\Psi_1 - \Psi_0 \right) - h_{-\frac{1}{2}} \left(\frac{\partial F_{in}}{\partial U_0} \right)^T \Psi_0 \\
C_1^{dadj} &= -\frac{1}{2} A_1^T \left(h_{\frac{3}{2}} \left(\Psi_2 - \Psi_1 \right) + h_{\frac{1}{2}} \left(\Psi_1 - \Psi_0 \right) \right) - h_{-\frac{1}{2}} \left(\frac{\partial F_{in}}{\partial U_1} \right)^T \Psi_0 \\
D_0^{dadj} &= -\kappa^{(2)}_{\frac{1}{2}} \Psi_1 + \kappa^{(4)}_{\frac{3}{2}} \left(\Psi_2 - \Psi_1 \right) - \kappa^{(4)}_{\frac{1}{2}} \left(\Psi_1 - \Psi_0 \right) \\
D_1^{dadj} &= -\kappa^{(2)}_{\frac{3}{2}} (\Psi_2 - \Psi_1) + \kappa^{(2)}_{\frac{1}{2}} \Psi_1 + (\kappa^{(4)}_{\frac{5}{2}} \Psi_3 - 3\kappa^{(4)}_{\frac{3}{2}} \Psi_2 + 2\kappa^{(4)}_{\frac{1}{2}} \Psi_1) \\
&\quad - (\kappa^{(4)}_{\frac{5}{2}} \Psi_2 - 3\kappa^{(4)}_{\frac{3}{2}} \Psi_1 + 2\kappa^{(4)}_{\frac{1}{2}} \Psi_0)
\end{aligned}
\tag{46}
$$

and

Exit

$$
\begin{aligned}
C_{n_e-1}^{dadj} &= -\frac{1}{2} A_{n_e-1}^T h_{n_e-\frac{3}{2}} \left(\Psi_{n_e-1} - \Psi_{n_e-2} \right) + h_{n_e-\frac{1}{2}} \left(\frac{\partial F_{out}}{\partial U_{n_e-1}} \right)^T \Psi_{n_e-1} \\
C_{n_e-2}^{dadj} &= -\frac{1}{2} A_{n_e-2}^T \left(h_{n_e-\frac{3}{2}} \left(\Psi_{n_e-1} - \Psi_{n_e-2} \right) + h_{n_e-\frac{5}{2}} \left(\Psi_{n_e-2} - \Psi_{n_e-3} \right) \right) + h_{n_e-\frac{1}{2}} \left(\frac{\partial F_{out}}{\partial U_{n_e-2}} \right)^T \Psi_{n_e-1} \\
D_{n_e-1}^{dadj} &= -\kappa^{(2)}_{n_e-\frac{3}{2}} \Psi_{n_e-2} + \kappa^{(4)}_{n_e-\frac{3}{2}} \left(\Psi_{n_e-1} - \Psi_{n_e-2} \right) - \kappa^{(4)}_{n_e-\frac{5}{2}} \left(\Psi_{n_e-2} - \Psi_{n_e-3} \right) \\
D_{n_e-2}^{dadj} &= -\kappa^{(2)}_{n_e-\frac{5}{2}} (\Psi_{n_e-3} - \Psi_{n_e-2}) + \kappa^{(2)}_{n_e-\frac{3}{2}} \Psi_{n_e-2} + (\kappa^{(4)}_{n_e-\frac{7}{2}} \Psi_{n_e-4} - 3\kappa^{(4)}_{n_e-\frac{5}{2}} \Psi_{n_e-3} + 2\kappa^{(4)}_{n_e-\frac{3}{2}} \Psi_{n_e-2}) \\
&\quad - (\kappa^{(4)}_{n_e-\frac{7}{2}} \Psi_{n_e-3} - 3\kappa^{(4)}_{n_e-\frac{5}{2}} \Psi_{n_e-2} + 2\kappa^{(4)}_{n_e-\frac{3}{2}} \Psi_{n_e-1})
\end{aligned}
\tag{47}
$$

For future convenience we note that, in view of the definition of the in/out states in Eqs. (30) and (31), the in/out Jacobians can be written as

$$\frac{\partial F_{in}}{\partial U_0} = 2\left.\frac{\partial F}{\partial M}\right|_{U_{in}} \left.\frac{\partial M}{\partial U}\right|_{U_0},$$

$$\frac{\partial F_{in}}{\partial U_1} = -\left.\frac{\partial F}{\partial M}\right|_{U_{in}} \left.\frac{\partial M}{\partial U}\right|_{U_1},$$

and (48)

$$\frac{\partial F_{out}}{\partial U_{n_e-1}} = 2\left(\left.\frac{\partial F}{\partial \rho}\right|_{U_{out}} \left.\frac{\partial \rho}{\partial U}\right|_{U_{n_e-1}} + \left.\frac{\partial F}{\partial u}\right|_{U_{out}} \left.\frac{\partial u}{\partial U}\right|_{U_{n_e-1}} \right),$$

$$\frac{\partial F_{out}}{\partial U_{n_e-2}} = -\left(\left.\frac{\partial F}{\partial \rho}\right|_{U_{out}} \left.\frac{\partial \rho}{\partial U}\right|_{U_{n_e-2}} + \left.\frac{\partial F}{\partial u}\right|_{U_{out}} \left.\frac{\partial u}{\partial U}\right|_{U_{n_e-2}} \right)$$

respectively.

5. RESULTS

5.1. Validation

The test case considered for the present study is the subsonic isentropic flow through a converging-diverging nozzle with cross section distribution given by [9,15]

$$h(x) = \begin{cases} 2 & -1 \le x \le 0.5 \\ 1+\sin^2(\pi x) & -0.5 \le x \le 0.5 \\ 2 & 0.5 \le x \le 1 \end{cases} \tag{49}$$

Total pressure and enthalpy remain constant throughout the duct and are defined to give a Mach number at the inlet equal to 0.12. A comparison between the analytic flow solution (obtained from the Mach-Area relation) and the numerical solution obtained on a uniform grid with 100 cells is displayed in Fig. 2 for the Mach number distribution, showing that the agreement is quite good.

The numerical solution of the adjoint problem obtained with the continuous approach is shown in Fig. 3. In this figure, the analytic solution obtained with the Green´s function approach of Giles and Pierce [9] is also shown. The agreement between both solutions is within numerical accuracy, showing that the dissipation model for the adjoint equations, which is formulated in an ad hoc manner, is suitable at least for subsonic flows. Several tests have been carried out in order to see both the influence of the fourth order dissipation level (k_4) and the order of extrapolation at the boundaries (Eq. (39)) showing that the continuous adjoint solution is quite insensitive to both.

The numerical discrete adjoint solution is compared against the analytic adjoint solution in Fig. 4. Although the discrete solution is qualitatively similar to the analytic one, there is an appreciable shift in the solution levels. In addition, there is a strong oscillation in the second adjoint variable at the exit. We have noticed that these oscillations can be eliminated by increasing the artificial dissipation (k_4) or, alternatively, the number of grid points, both of which also improve the quality of the solution (Fig. 5). Nevertheless, the authors have been surprised by the results obtained using the discrete approach since it can be shown that the convective and dissipative terms are essentially the same as in the continuous adjoint approach, the only difference between the two approaches lying in the boundary terms. The influence of the formulation of the boundary conditions on the discrete adjoint solutions has been observed before [13,16,17]. We will come back to this issue below.

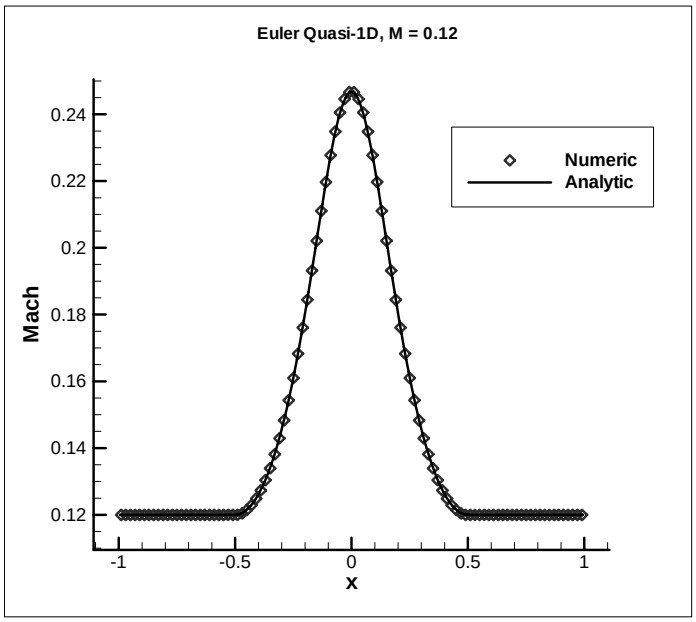

Fig. 2. Mach number distribution for the converging-diverging nozzle (49) under subsonic flow conditions. M_{in} = 0.12.

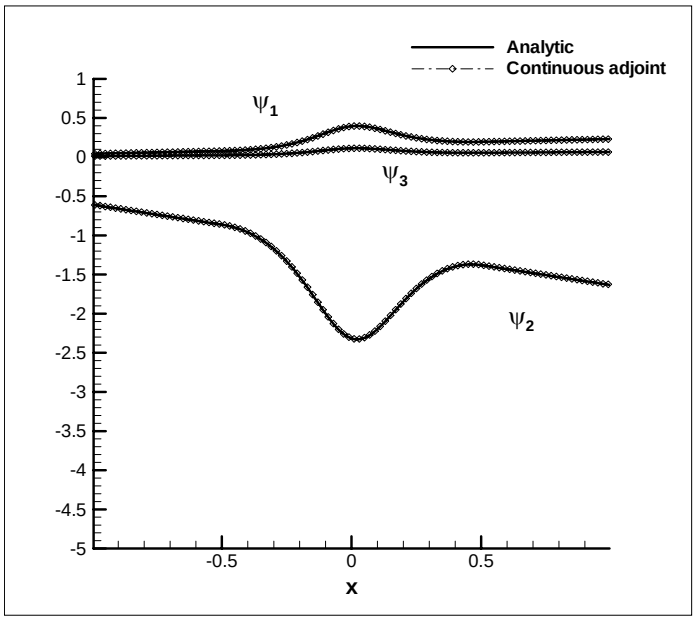

Fig. 3. Continuous Adjoint solution for the converging-diverging nozzle (49) under subsonic flow conditions. M_{in} = 0.12.

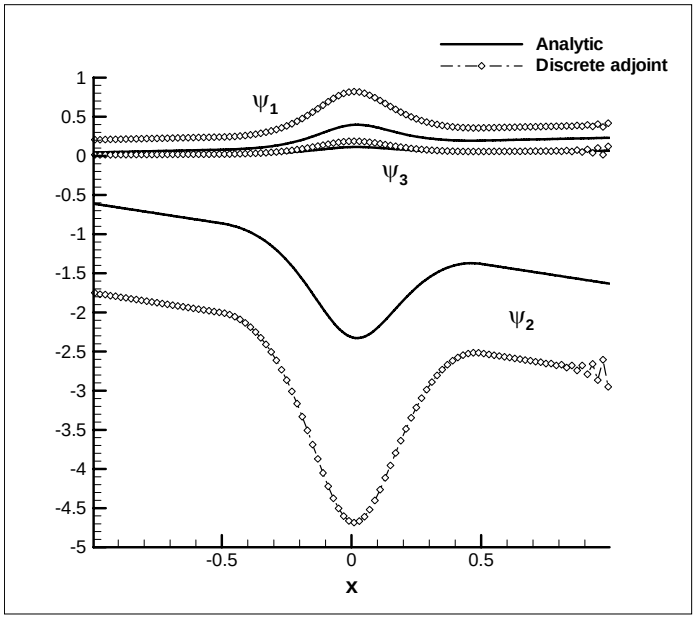

Fig. 4. Discrete adjoint solution for the converging-diverging nozzle (49) under subsonic flow conditions. M_{in} = 0.12.

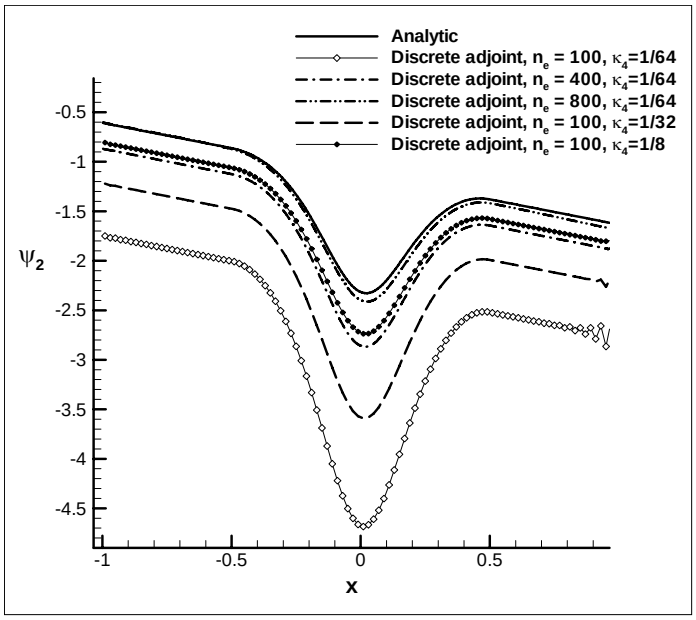

Fig. 5. Influence of artificial dissipation and grid spacing on the discrete adjoint solution for the converging-diverging nozzle (49) under subsonic flow conditions. M_{in} = 0.12.

7.2. Effect of the extrapolation order

To further investigate the origin of the discrepancy between the discrete and continuous adjoint solutions, we recall the expressions for their respective residuals at the inlet/exit boundaries, given in Eqs. (37), (38) and (46), (47). We restrict ourselves to the convective part of the residuals, which numerical testing show to be the only relevant one for the problem at hand.

j	Continuous Adj.	Discrete Adj.
0	$\frac{1}{2}A_0^T h_{\frac{1}{2}}\left(\Psi_1-\Psi_0\right)+A_0^T h_{-\frac{1}{2}}\left(\Psi_1-\Psi_0\right)$ $+h_{-\frac{1}{2}}\frac{\partial M}{\partial U}^T\left(\frac{\partial F}{\partial M}^T\cdot(2\Psi_0-\Psi_1)\right)$	$\frac{1}{2}A_0^T h_{\frac{1}{2}}\left(\Psi_1-\Psi_0\right)+2h_{-\frac{1}{2}}\frac{\partial M}{\partial U}\Big\vert_{U_0}^T\frac{\partial F}{\partial M}\Big\vert_{U_{in}}^T\cdot\Psi_0$
1	$\frac{1}{2}A_1^T h_{\frac{3}{2}}\left(\Psi_2-\Psi_1\right)+\frac{1}{2}A_1^T h_{\frac{1}{2}}\left(\Psi_1-\Psi_0\right)$	$\frac{1}{2}A_1^T h_{\frac{3}{2}}\left(\Psi_2-\Psi_1\right)+\frac{1}{2}A_1^T h_{\frac{1}{2}}\left(\Psi_1-\Psi_0\right)$ $-h_{-\frac{1}{2}}\frac{\partial M}{\partial U}\Big\vert_{U_1}^T\frac{\partial F}{\partial M}\Big\vert_{U_{in}}^T\cdot\Psi_0$
n_e-2	$\frac{1}{2}A_{n_e-2}^T h_{n_e-\frac{3}{2}}\left(\Psi_{n_e-1}-\Psi_{n_e-2}\right)$ $+\frac{1}{2}A_{n_e-2}^T h_{n_e-\frac{5}{2}}\left(\Psi_{n_e-2}-\Psi_{n_e-3}\right)$	$\frac{1}{2}A_{n_e-2}^T\left(h_{n_e-\frac{3}{2}}\left(\Psi_{n_e-1}-\Psi_{n_e-2}\right)+h_{n_e-\frac{5}{2}}\left(\Psi_{n_e-2}-\Psi_{n_e-3}\right)\right)$ $+h_{n_e-\frac{1}{2}}\left(\frac{\partial\rho}{\partial U}\Big\vert_{U_{n_e-2}}^T\frac{\partial F}{\partial\rho}\Big\vert_{U_{out}}^T+\frac{\partial u}{\partial U}\Big\vert_{U_{n_e-2}}^T\frac{\partial F}{\partial u}\Big\vert_{U_{out}}^T\right)\cdot\Psi_{n_e-1}$

n_e-1	$\frac{1}{2}A^T_{n_e-1}h_{n_e-\frac{3}{2}}\left(\Psi_{n_e-1}-\Psi_{n_e-2}\right)$ $+A^T_{n_e-1}h_{n_e-\frac{1}{2}}\left(\Psi_{n_e-1}-\Psi_{n_e-2}\right)$ $-2h_{n_e-\frac{1}{2}}\left(\frac{\partial\rho}{\partial U}^T\frac{\partial F}{\partial\rho}^T+\frac{\partial u}{\partial U}^T\frac{\partial F}{\partial u}^T\right)\cdot\Psi_{n_e-1}$ $+h_{n_e-\frac{1}{2}}\left(\frac{\partial\rho}{\partial U}^T\frac{\partial F}{\partial\rho}^T+\frac{\partial u}{\partial U}^T\frac{\partial F}{\partial u}^T\right)\cdot\Psi_{n_e-2}$	$\frac{1}{2}A^T_{n_e-1}h_{n_e-\frac{3}{2}}\left(\Psi_{n_e-1}-\Psi_{n_e-2}\right)$ $-2h_{n_e-\frac{1}{2}}\left(\left.\frac{\partial\rho}{\partial U}\right\|^T_{U_{n_e-1}}\left.\frac{\partial F}{\partial\rho}\right\|^T_{U_{out}}+\left.\frac{\partial u}{\partial U}\right\|^T_{U_{n_e-1}}\left.\frac{\partial F}{\partial u}\right\|^T_{U_{out}}\right)\cdot\Psi_{n_e-1}$

where for the continuous adjoint residual we have considered a first-order extrapolation $\Psi^{(e)}_{in}=2\Psi_{j=0}-\Psi_{j=1}$ and $\Psi^{(e)}_{out}=2\Psi_{j=n_e-1}-\Psi_{j=n_e-2}$, respectively. Notice that the discrete convective fluxes are similar to the continuous ones, except for what can be interpreted as a decrease in the extrapolation order of the discrete adjoint variables. In fact, the following ad hoc modification of the boundary discrete adjoint residuals

$$
\begin{aligned}
R_0^{dadj,new} &= \frac{1}{2}A_0^T h_{\frac{1}{2}}\left(\Psi_1-\Psi_0\right)+h_{-\frac{1}{2}}\left.\frac{\partial M}{\partial U}\right|^T_{U_0}\left.\frac{\partial F}{\partial M}\right|^T_{U_{in}}\cdot(2\Psi_0-\Psi_1)\\
R_{n_e-1}^{dadj,new} &= \frac{1}{2}A^T_{n_e-1}h_{n_e-\frac{3}{2}}\left(\Psi_{n_e-1}-\Psi_{n_e-2}\right)\\
&-h_{n_e-\frac{1}{2}}\left(\left.\frac{\partial\rho}{\partial U}\right|^T_{U_{n_e-1}}\left.\frac{\partial F}{\partial\rho}\right|^T_{U_{out}}+\left.\frac{\partial u}{\partial U}\right|^T_{U_{n_e-1}}\left.\frac{\partial F}{\partial u}\right|^T_{U_{out}}\right)\cdot(2\Psi_{n_e-1}-\Psi_{n_e-2})
\end{aligned}
\tag{50}
$$

(which amounts, roughly speaking, to an increase of the extrapolation order of the adjoint variables) does correct the discrete adjoint solution, as can be seen in Fig. 6. Notice that to obtain such modified residuals within the discrete adjoint solver, while keeping it discretely adjoint to the flow solver, it is necessary to modify the flow solver discretization by (somewhat unnaturally) inserting $F(U_{in})$ (resp. $F(U_{out})$) into the next-to-boundary cell residuals R_1 (resp. R_{n_e-2}), as follows

$$
\begin{aligned}
R_1 &\to R_1-\frac{1}{2}h_{-\frac{1}{2}}F(U_{in})\\
R_{n_e-2} &\to R_{n_e-2}+\frac{1}{2}h_{n_e-\frac{1}{2}}F(U_{out})
\end{aligned}
\tag{51}
$$

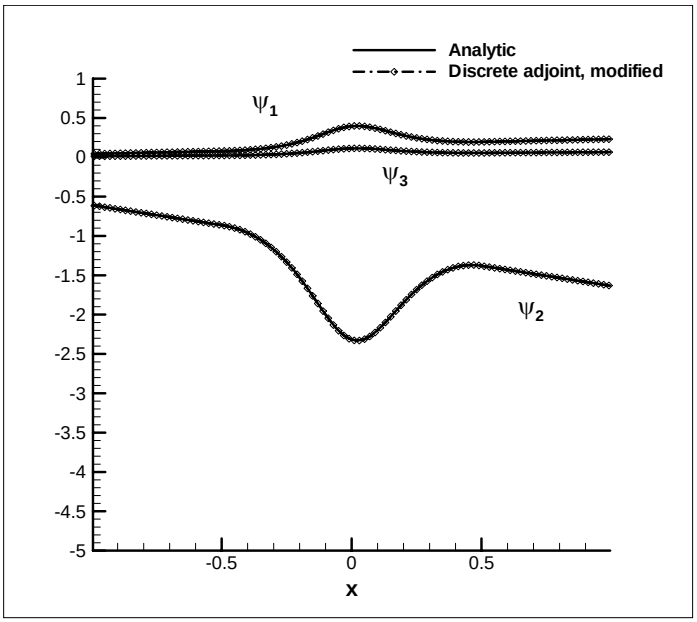

Fig. 6. Effect of boundary residual modification on the discrete adjoint solution (n_e = 100) for the converging-diverging nozzle (49) under subsonic flow conditions. M_{in} = 0.12.

To close this analysis it is instructive to examine the continuous limit of the above residuals. In the limit where the grid spacing dx goes to zero, the boundary residuals behave as

j	Continuous Adj.	Discrete Adj.
0	$\left(h\left(\frac{3}{2}A^T - \frac{\partial M}{\partial U}^T \frac{\partial F}{\partial M}^T \right) \frac{d\Psi}{dx}\Big\|_{x=-1} \right) dx + h \frac{\partial M}{\partial U}^T \frac{\partial F}{\partial M}^T \cdot \Psi(-1)$	$-\frac{1}{2} h A^T \frac{d\Psi}{dx}\Big\|_{x=-1} dx + 2h \frac{\partial M}{\partial U}^T \frac{\partial F}{\partial M}^T \cdot \Psi(-1)$
n_e-1	$h\left(\frac{3A^T}{2} - \left(\frac{\partial \rho}{\partial U}^T \frac{\partial F}{\partial \rho}^T + \frac{\partial u}{\partial U}^T \frac{\partial F}{\partial u}^T \right) \right) \frac{d\Psi}{dx}\Big\|_{x=1} dx - h\left(\frac{\partial \rho}{\partial U}^T \frac{\partial F}{\partial \rho}^T + \frac{\partial u}{\partial U}^T \frac{\partial F}{\partial u}^T \right) \Psi(1)$	$\frac{1}{2} h A^T \frac{d\Psi}{dx}\Big\|_{x=1} dx - 2h \left(\frac{\partial \rho}{\partial U}^T \frac{\partial F}{\partial \rho}^T + \frac{\partial u}{\partial U}^T \frac{\partial F}{\partial u}^T \right) \cdot \Psi(1)$

As the mesh width is reduced, all the above residuals must vanish, so the terms which escalate as dx^0 must vanish identically. One then consistently recovers the continuous adjoint boundary conditions as stated in equations (15) and (21).

7.3. Sample sensitivity computation

To test the influence of the accuracy of the numerical adjoint solutions on sensitivity computations, we investigate a shape optimization problem using a set of Hicks-Henne bump functions superimposed on the baseline duct shape as

$$\tilde{h}(x) = h(x) + f_k(x) \tag{52}$$

The design variables are the weights α_k multiplying each Hicks-Henne function

$$f_k(x) = \alpha_k \left(\sin\left(\pi x^{\frac{\log 0.5}{\log x_k}} \right) \right)^n \tag{53}$$

where x_k locates the maximum of the bump at $x = x_k$, and n controls the width of the bump. In the cases considered, $n = 3$ and the maxima x_k are evenly distributed along the near-throat region $-0.5 \le x \le 0.5$. Fig. 7 shows a comparison between the derivatives computed with the continuous adjoint approach (as per Eq. (12)), with the discrete adjoint approach, which is computed as

$$\frac{\partial J}{\partial \alpha_k} = \sum_{j=0}^{n_e-1} \Psi_j^T \left(\frac{R_j(U, h + f_k) - R_j(U, h)}{\alpha_k} \right) \tag{54}$$

(where $R_j(U, h + f_k)$ and $R_j(U, h)$ are the discrete residuals calculated at the original geometry and at the geometry perturbed in the *k*-th design direction, both with the *unperturbed* flow solution) and via finite-differences. In addition, derivatives are also shown from a "hybrid" approach in which the adjoint variables are obtained from the continuous adjoint approach and are subsequently used in a discrete adjoint framework to compute the sensitivity derivatives by using Eq. (54). The accuracy of the derivatives using either adjoint approach is comparable to that obtained via finite-differences, although the discrete and hybrid approaches tend to outperform the purely continuous approach.

In these numerical experiments, all results are sufficiently converged (up to a seven-order-of-magnitude drop in the residuals in all cases) and the step size for computing the finite-difference derivatives has been varied over a large range of values with no significant changes in the results.

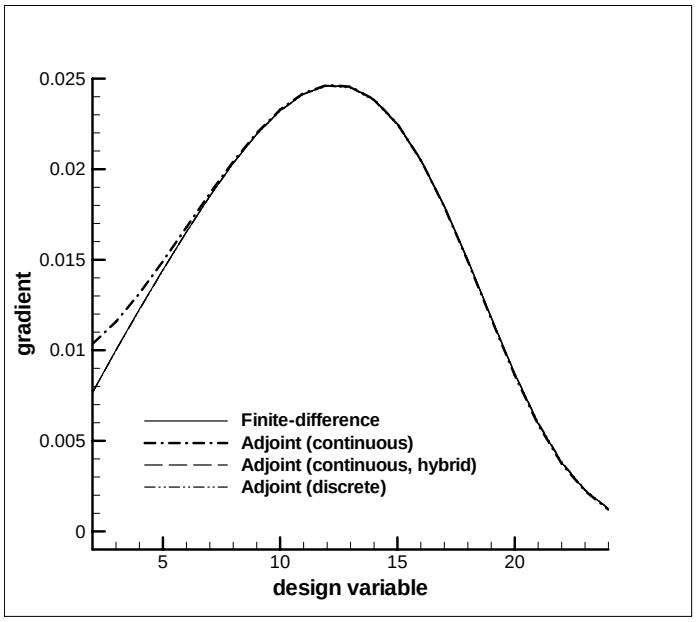

Fig. 7. Comparison of sensitivity derivatives (n_e = 100) for the converging-diverging nozzle (49) under subsonic flow conditions. M_{in} = 0.12.

8. CONCLUSIONS

In this study, we have undertaken a detailed description of the procedure to obtain the adjoint solutions of the quasi-one dimensional Euler equations from the analytical and numerical points of view. A comparison between the continuous and discrete approaches has been carried out. For the continuous adjoint approach, a systematic procedure for dealing with the implementation of boundary conditions on numerical solvers has been presented, which clearly specifies which adjoint variables (or combinations thereof) are to be extrapolated and which ones prescribed so as to respect the analytic boundary conditions. While the continuous adjoint approach, with the appropriate boundary conditions, which must be derived in a case-by-case basis, gives a fairly accurate solution even on relatively coarse meshes, the solutions obtained with the discrete adjoint approach are not satisfactory with the present implementation of the discrete boundary treatment, which is automatically inherited from the discretization scheme of the flow solver. Getting a reasonably accurate discrete adjoint solution requires either too fine a mesh, or a change in the discretization algorithm, which in turns requires changing the discretization algorithm of the flow solver. While these results are probably anecdotic and difficult to extrapolate to more general settings, an important lesson can be drawn from them: the continuous adjoint approach, while lacking in flexibility concerning the boundary conditions, offers more flexibility when it

comes to modifying the numerical scheme, which can be done independently of the flow solver. The discrete adjoint approach, in turn, lifts the burden of the derivation of the adjoint boundary conditions, but its structure is rigidly tied to that of the flow solver, which complicates the process of algorithm modification. Whenever the resulting discrete adjoint numerical scheme turns out to be inefficient or inaccurate, its modification requires double coding and double validation, especially if differentiation of the primal solver is performed by hand.

In spite of the inaccuracy of the discrete adjoint solution, the sensitivity derivatives turn out to be surprisingly accurate even on fairly coarse grids. On the one hand, this is good news as far as design processes are concerned, since it shows that the cost function gradients are rather insensitive to the accuracy of the adjoint solutions; on the other hand, it shows that validating the adjoint solutions on the basis of the gradients alone, which is common practice owing to the lack of exact adjoint solutions for problems of industrial interest, can overlook inaccuracies in the solution or coding flaws in the adjoint solver.

ACKNOWLEDGEMENTS

This work has been supported in part by the Spanish ministry of Defence/INTA under the activity “Termofluidodinámica” (IGB99001).

REFERENCES

[1] Jameson, A., "Aerodynamic Design Via Control Theory," *Journal of Scientific Computing*, Vol. 3, 1988, pp. 233–260.
[2] Jameson, A., "Optimum Aerodynamic Design Using CFD And Control Theory," *AIAA Paper 95–1729*, 1995.
[3] Jameson, A., Pierce, N., and Martinelli, L., "Optimum Aerodynamic Design using the Navier-Stokes Equation," *Theoretical and Computational Fluid Dynamics*, Vol. 10, 1998, pp. 213–237.
[4] Castro, C., Lozano, C., Palacios, F., and Zuazua, E., "Systematic Continuous Adjoint Approach to Viscous Aerodynamic Design on Unstructured Grids," *AIAA Journal*, Vol. 45, No. 9, September 2007, pp. 2125–2139.
[5] Giles, M. B. and Pierce, N. A., "Adjoint error correction for integral outputs," in *Error estimation and solution adaptive discretization in computational fluid dynamics*, T. Barth and H. Deconinck, (eds.), Lecture Notes in Computer Science and Engineering, vol.25. Springer Verlag, Berlin, 2002.
[6] Giles, M. B. and Pierce, N. A., "Adjoint recovery of superconvergent functionals from approximate solutions of partial differential equations," Oxford University Computing Laboratory Report, no. NA-98/18, 1998.

[7] Giles, M. B., Pierce, N. A., and Süli, E., "Progress in adjoint error correction for integral functionals," *Computing and Visualisation in Science*, Vol. 6, No. 2–3, 2004.
[8] Nadarajah, S., and Jameson, A., "A Comparison of the Continuous and Discrete Adjoint Approach to Automatic Aerodynamic Optimization," *AIAA paper 2000–0667, 38th AIAA Aerospace Sciences Meeting and Exhibit*, Reno, NV, January 2000.
[9] Giles, M. and Pierce, N., "Analytic adjoint solutions for the quasi-one-dimensional Euler equations," *J. Fluid Mechanics*, Vol. 426, 2001, pp. 327–345.
[10] Giles, M. B. and Pierce, N. A., "Adjoint Equations in CFD: Duality, Boundary Conditions and Solution Behavior," *AIAA Paper 97–1850*, 1997.
[11] Xie, L., *Gradient-Base Optimum Aerodynamic Design Using Adjoint Methods*, Ph.D. Thesis, Virginia Polytechnic Institute, 2002.
[12] Duivesteijn, G. F., Bijl, H., Koren, B., and Brummelen, E. H. v., "Comparison of two adjoint equation approaches with respect to boundary-condition treatments for the quasi-1D Euler equations," *ADMOS 2003, International Conference on Adaptive Modeling and Simulation*, CIMNE, Barcelona, 2003, N.-E. Wiberg and P. Díez, (eds.).
[13] Duivesteijn, G. F., Bijl, H., Koren, B., and Brummelen, E. H. v., "On the adjoint solution of the quasi-1D Euler equations: the effect of boundary conditions and the numerical flux function," *Int. J. Numer. Meth. Fluids*, Vol. 47, 2005, pp. 987–993.
[14] Jameson, A., Schmidt, W., and Turkel, E., "Numerical solution of the Euler equations by finite volume methods using Runge-Kutta time stepping schemes," *AIAA Paper*, Vol. 81, 1981, pp. 1259.
[15] Giles, M. B. and Pierce, N. A., "On the properties of solutions of the adjoint Euler equations," *6th ICFD Conference on Numerical Methods for Fluid Dynamics*, Oxford, UK, 1998.
[16] Anderson, W. K. and Venkatakrishnan, V., "Aerodynamic Design Optimization on Unstructured Grids with a Continuous Adjoint Formulation," *Computers and Fluids*, Vol. 28, 1999, pp. 443–480.
[17] Giles, M. B., Duta, M. C., Müller, J.-D., and Pierce, N. A., "Algorithm Developments for Discrete Adjoint Methods," *AIAA Journal*, Vol. 41, No. 2, 2003, pp. 198-205.